

Effectively Restricting MnSi Precipitates for Simultaneously Enhancing the Seebeck Coefficient and Electrical Conductivity in Higher Manganese Silicide

*Wei-Di Liu,^a Xiao-Lei Shi,^a Raza Moshwan,^a Qiang Sun,^a Lei Yang,^c Zhi-Gang Chen^{*b,a} Jin
Zou^{*a,d}*

^aMaterials Engineering, the University of Queensland, Brisbane, Queensland 4072, Australia.

^bCentre for Future Materials, the University of Southern Queensland, Springfield, Queensland
4300, Australia.

^cSchool of Materials Science and Engineering, the Sichuan University, Chengdu 610065, China.

^dCentre for Microscopy and Microanalysis, the University of Queensland, Brisbane, Queensland
4072, Australia.

1. Experimental details

Material preparation: The higher manganese silicide with different amount of additional Mg₂Si (MnSi_{1.73} + x% Mg₂Si, x = 0, 1, 3 and 5) were synthesized with Manganese powders (99%), silicon powders (99%) and Mg₂Si powders (99%) purchased from Sigma Aldrich. In a typical synthesis, the Mn, Si and Mg₂Si powders were weighed as the designed amount and flame sealed in a silica

tube which has been pre-evacuated to 0 Pa. The silica tubes were subsequently loaded into a Muffle furnace, heated to 1473 K, dwelled for 24 h and slowly cooled to room-temperature. The obtained ingots were subsequently ball-milled into powders with tungsten carbide jars and balls in SPEX 8000M for only 30 min. The obtained powders were then spark plasma sintered (211Lx) into pellets under vacuum at 1073 K and 50 MPa.

Thermoelectric performance measurement: The σ and S of as-sintered pellets were measured in ZEM3, simultaneously. The κ was calculated as $\kappa = \rho \cdot C_p \cdot D$, the ρ , C_p and D the sample density, specific heat and thermal diffusivity, respectively. The ρ of all sintered pellets were measured by Archimedes method and are higher than 97%, as shown in **Table S1 (Table R1)**. The theoretical ρ is taken as 5.16 g cm⁻³. The C_p was measured by DSC 404 F3 (NETZSCH). The D was measured by LFA 467 (HyperFlash, NETZSCH). To understand the carrier transport properties, room-temperature n_H was measured by the van der Pauw technique under a reversible magnetic field. All thermoelectric performance was measured perpendicular to the pressing direction.

Table S1. Densities of as-sintered MnSi_{1.73+x%Mg₂Si} ($x=0, 1, 3$ and 5) pellets.

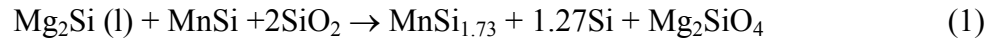
Sample	MnSi _{1.73}	MnSi _{1.73+1%Mg₂Si}	MnSi _{1.73+3%Mg₂Si}	MnSi _{1.73+5%Mg₂Si}
Density (g cm ⁻³)	5.01	5.05	5.04	5.02
Relative Density	97%	98%	98%	97%

Structural Characterization: The room-temperature structural information of as-sintered pellets were collected by a Bruker D8 advanced powder X-ray diffraction (XRD) with graphite monochromatized Cu K α radiation source ($\lambda = 0.15408$ nm). The composition was analyzed via

energy dispersive X-ray spectroscopy (EDS, Hitachi SU3500). The crystal structure was further confirmed by Transmission electron microscopy (Philips Tecnai F20 FEG-S/TEM) on a specimen cut from the sintered pellet ($\text{MnSi}_{1.73} + 5\% \text{Mg}_2\text{Si}$) by Ultramicrotone.

2. The influence of Mg_2Si addition on MnSi removal

As Mn and Si should form solid solution under the reaction temperature, the possible reason for additional Mg_2Si helping remove MnSi impurities is the reaction between Mg_2Si , MnSi impurity and the silica tube under high temperature during the cooling process when MnSi precipitate,



which has introduced additional Si into the solid solution at high temperature and thus restrained the precipitation of MnSi. Furthermore, the additional Si should form at where MnSi precipitates. They could possibly restrain the precipitation of MnSi more effectively than simply introducing additional Si. Meanwhile, the additional Si (considering the Si amount introduced due to additional Mg_2Si ($\leq 5\%$)) should have further reacted with the $\text{MnSi}_{1.73}$ and formed solid solution:



where the estimated composition of the solid solution is consistent with other studies.¹

3. MnSi phase in as-sintered $\text{MnSi}_{1.73}$ pellet

To further verify the existence of MnSi precipitates in $\text{MnSi}_{1.73}$ sample without additional Mg_2Si , we made SEM-EDS analysis of as-sintered $\text{MnSi}_{1.73}$ pellet and the results are shown in **Figure S1**. **Figure S1a** shows a SEM-BSE image, where the bright areas are the MnSi precipitates with heavier average atomic number. **Figure S1b** shows the corresponding EDS spectra on spot 1 and 2 of **Figure S1a** as well as relative quantitative analyses results. As can be seen, the bright areas have a Mn/Si ratio close to 1, indicating that the bright phase is MnSi, which is consistent with the XRD result. The matrix material has a higher Si/Mn ratio as being the HMS. **Figure S1c** shows

the corresponding EDS line scan results, indicating that the bright areas are Si-insufficient and Mn-rich. On this basis, it can be concluded that the bright area should be MnSi precipitates.

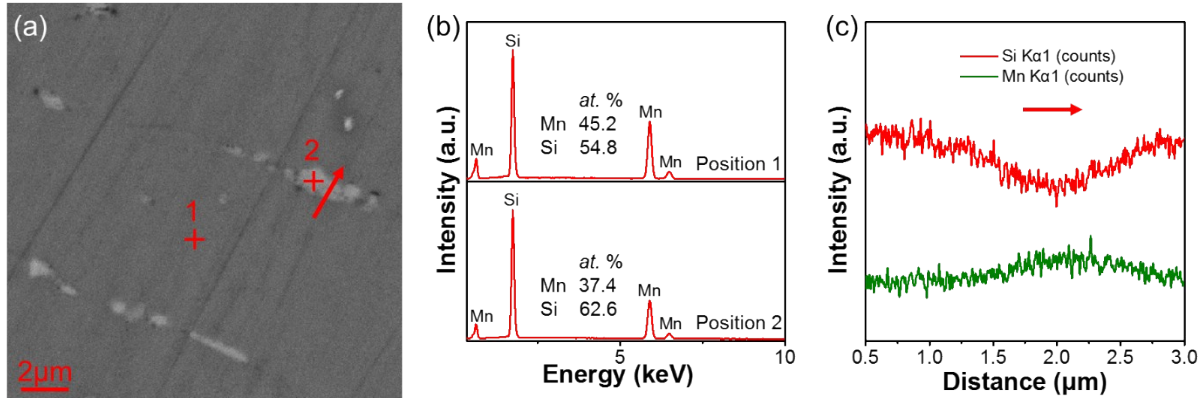


Figure S1. (a) SEM-BSE image of as-sintered MnSi_{1.73} pellet, (b) EDS spectrum on point 1 and 2 of (a) as well as the quantitative analysis results and (c) EDS line scan result along the direction as shown by the arrow in (a).

4. The influence of additional Mg₂SiO₄ on the thermoelectric performance of MnSi_{1.73}

Figure S2 plots temperature-dependent thermoelectric performance of the as-sintered MnSi_{1.73} + 5% Mg₂SiO₄ pellet in comparison with the high purity HMS synthesized by similar high-temperature methods.²⁻⁴ As can be seen, with additional Mg₂SiO₄, thermoelectric performance of the MnSi_{1.73} + 5% Mg₂SiO₄ pellet is roughly consistent with those high purity ones by others. Regardless of the slight difference between σ , S and κ , the zT value of our MnSi_{1.73} + 5% Mg₂SiO₄ pellet with additional Mg₂SiO₄ is comparable with those high purity HMS samples.

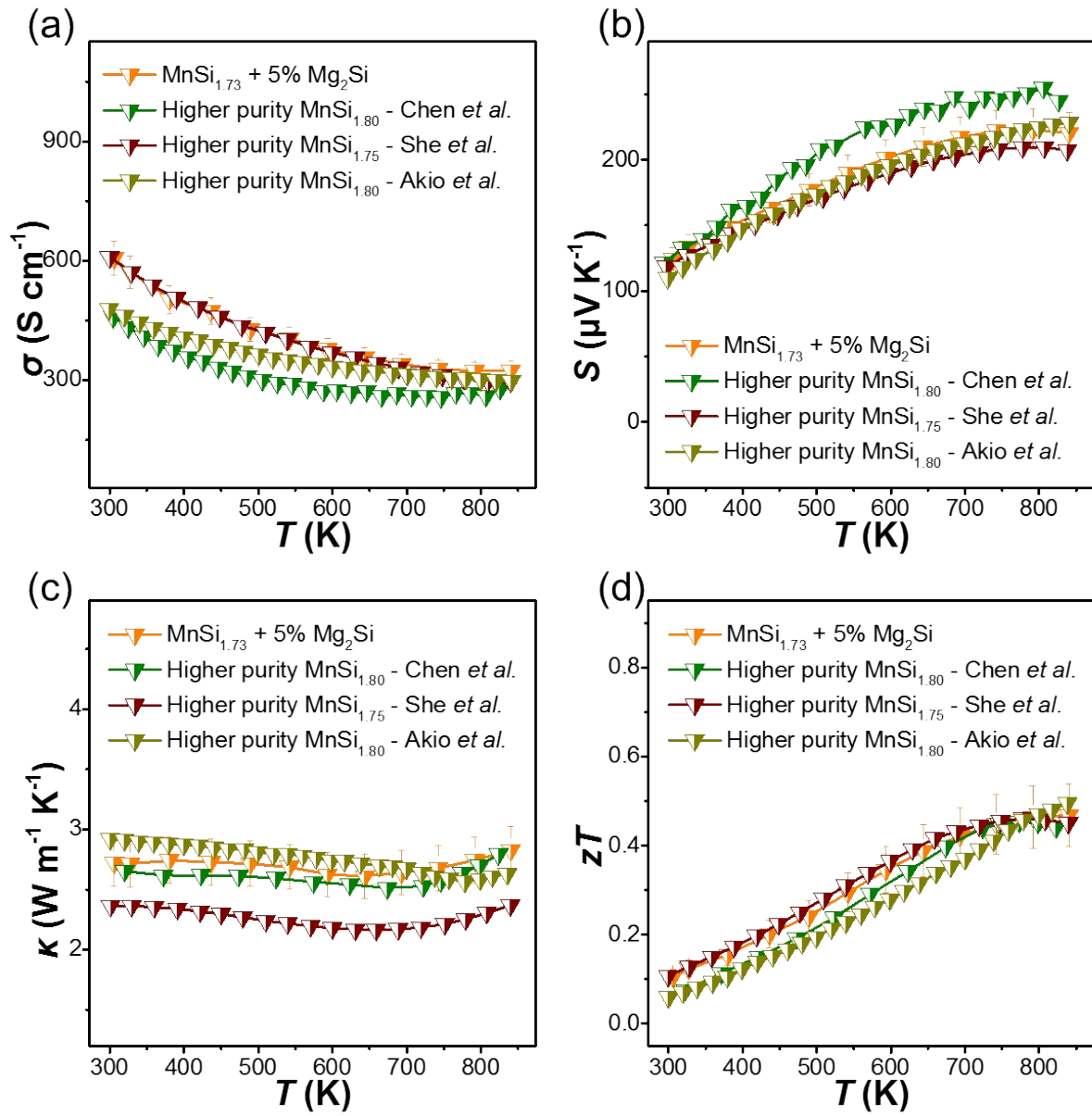


Figure S2. Temperature-dependent thermoelectric performance of as-sintered $\text{MnSi}_{1.73} + 5\%$ Mg_2Si pellet in comparison with the high purity ones: (a) σ , (b) S , (c) κ and (d) zT .²⁻⁴

Reference

1. W. H. Luo, H. Li, Z. B. Lin and X. F. Tang, *Acta Phys. Sin-ch. Ed.*, 2010, **59**, 8783-8788.
2. X. She, X. Su, H. Du, T. Liang, G. Zheng, Y. Yan, R. Akram, C. Uher and X. Tang, *J. Mater. Chem. C*, 2015, **3**, 12116-12122.
3. X. Chen, S. N. Girard, F. Meng, E. Lara-Curzio, S. Jin, J. B. Goodenough, J. Zhou and L. Shi, *Adv. Energy Mater.*, 2014, **4**, 1-10.
4. Y. Akio, G. Swapnil, M. Hidetoshi, I. Manabu, N. Yoichi, M. Masaharu and T. Tsunehiro, *Jpn. J. Appl. Phys.*, 2016, **55**, 020301.